ARTICLE

Increased CXCL10 (IP-10) is associated with advanced myeloproliferative neoplasms and its loss dampens erythrocytosis in mouse models

Miriam Belmonte[a,b], Lilia Cabrera-Cosme[c], Nina F. Øbro[a,b], Juan Li[a,b], Jacob Grinfeld[a,b,d], Joanna Milek[c], Ellie Bennett[c], Melissa Irvine[a,b], Mairi S. Shepherd[a,b], Alyssa H. Cull[a,b], Grace Boyd[c], Lisa M. Riedel[a,b], James Lok Chi Che[a,b,c], Caroline A. Oedekoven[a,b], E. Joanna Baxter[d], Anthony R. Green[a,b,d], Jillian L. Barlow[c], and David G. Kent[a,b,c]*

[a]Wellcome Medical Research Council (MRC) Cambridge Stem Cell Institute, University of Cambridge, Cambridge, United Kingdom; [b]Department of Haematology, University of Cambridge, Cambridge, United Kingdom; [c]Department of Biology, Centre for Blood Research, York Biomedical Research Institute, University of York, York, United Kingdom; [d]Department of Haematology, Cambridge University Hospitals National Health Service (NHS) Foundation Trust, Cambridge, United Kingdom

Key studies in pre-leukemic disorders have linked increases in pro-inflammatory cytokines with accelerated phases of the disease, but the precise role of the cellular microenvironment in disease initiation and evolution remains poorly understood. In myeloproliferative neoplasms (MPNs), higher levels of specific cytokines have been previously correlated with increased disease severity (tumor necrosis factor-alpha [TNF-α], interferon gamma−induced protein-10 [IP-10 or CXCL10]) and decreased survival (interleukin 8 [IL-8]). Whereas TNF-α and IL-8 have been studied by numerous groups, there is a relative paucity of studies on IP-10 (CXCL10). Here we explore the relationship of IP-10 levels with detailed genomic and clinical data and undertake a complementary cytokine screen alongside functional assays in a wide range of MPN mouse models. Similar to patients, levels of IP-10 were increased in mice with more severe disease phenotypes (e.g., JAK2$^{V617F/V617F}$ TET2$^{-/-}$ double-mutant mice) compared with those with less severe phenotypes (e.g., CALR^{del52} or JAK2$^{+/V617F}$ mice) and wild-type (WT) littermate controls. Although exposure to IP-10 did not directly alter proliferation or survival in single hematopoietic stem cells (HSCs) in vitro, IP-10$^{-/-}$ mice transplanted with disease-initiating HSCs developed an MPN phenotype more slowly, suggesting that the effect of IP-10 loss was noncell-autonomous. To explore the broader effects of IP-10 loss, we crossed IP-10$^{-/-}$ mice into a series of MPN mouse models and showed that its loss reduces the erythrocytosis observed in mice with the most severe phenotype. Together, these data point to a potential role for blocking IP-10 activity in the management of MPNs. © 2024 International Society for Experimental Hematology. Published by Elsevier Inc. This is an open access article under the CC BY license (http://creativecommons.org/licenses/by/4.0/)

HIGHLIGHTS

- IP-10 correlates with disease severity and the presence of *JAK2* and *TET2* mutations
- Mouse models have similarly dysregulated IP-10 expression as patients
- IP-10 loss partially ameliorates the polycythemia phenotype in mouse models

High levels of inflammatory cytokines have been observed in a number of hematological malignancies [1−6] and several lines of evidence support the association of cytokine deregulation with pathogenesis, disease progression, and patient survival. Alongside this, increases in pro-inflammatory cytokines have been linked with adverse clinical outcomes in elderly individuals [7]. A dynamic interaction between malignant cells and their niche also exists, whereby the cellular microenvironment is altered by the presence of the leukemic cells, creating a positive feedback loop to promote disease development [8,9]. However, the specific roles of particular cell types or secreted molecules in the early stages of hematological malignancies are not well understood. This is further complicated by both immune cells and leukemia cells sharing a common origin in the primitive hematopoietic stem and progenitor cell (HSPC) compartment, thus making "cause" versus "consequence" difficult to disentangle.

Numerous recent studies have described an inflammatory microenvironment in myeloproliferative neoplasms (MPNs) [10−14], a group of clonal pre-leukemic stem cell disorders characterized by

alterations in mature blood cell production. Overproduction of a number of pro-inflammatory cytokines has been observed in patients with MPN, including tumor necrosis factor-alpha (TNF-α) [15,16], IL-8 [2,17,18], and chemokine interferon gamma inducible protein of 10 kDa (CXCL10) [10], with the latter having relatively fewer subsequent investigations. CXCL10, also known as interferon gamma (IFN-γ)−induced protein-10 (IP-10), is a chemokine secreted in response to IFN-γ [19]. It binds the cell surface chemokine receptor C-X-C motif chemokine receptor 3 (CXCR3/CD183) that is present on a wide range of T and natural killer (NK) cell subsets [19].

In this study, we report a strong correlation of higher IP-10 levels with JAK2V617F, the most common driver mutation in MPNs, and *TET2* mutational status in both patients and mouse models with novel cellular sources of IP-10 in patients with more advanced disease. To explore its functional role, we crossed IP-10 knockout (KO) mice [20] with an allelic series of JAK2V617F knock-in (KI) and *Tet2* KO mice [21] and assessed its impact on red cell phenotypes associated with MPN pathogenesis.

METHODS

Primary Samples from Patients with MPN

This study used samples taken from 291 Philadelphia chromosome-negative patients with MPN, diagnosed according to British Committee for Standards in Haematology (BCSH) guidelines [22]. Peripheral blood (PB), serum, and bone marrow (BM) samples were obtained in accordance with the Declaration of Helsinki, under the approval of the Cambridge and Eastern Region Ethics Committee. Samples were taken at the time of the initial patient visit on referral to the specialist MPN clinic. Targeted sequencing of the coding regions of 33 recurrently mutated genes was available for 117 patients. To determine whether any of these mutations correlated with specific cytokine levels, patients were characterized for both JAK2V617F status and collaborating mutations by genetic sequencing or exome sequencing. In addition, clinical data were collected when available to correct for diagnosis, age, and sex.

Mice

All mice were maintained in the Central Biomedical Service (CBS) animal facility of Cambridge University or the Biological Services Facility (BSF) at the University of York. Both facilities are specific pathogen-free environments, and animals were cared for according to institutional guidelines. All mice were from a C57BL/6 background. Wild-type (WT) C57BL/6-Ly5.2 were purchased from Charles River Laboratories (Saffron Walden, Essex, UK). JAK2V617F KI (JAK) from Li et al. [23] mice, JAK2V617F/Tet2 KO (JAK TET) mice, and CALR Del52 (CALR) [24] mice were kindly provided by Anthony R. Green (University of Cambridge, UK) [25], and Tet2 KO (TET) mice were provided by Anjana Rao (La Jolla Institute for Immunology, La Jolla, CA, US) [26]. Homozygous B6.129S4-Cxcl10tm1Adl/J (IP-10 KO) were purchased from The Jackson Laboratory [20]. To generate double-mutant crosses (JAK TET), JAK2V617F KI mice were crossed with Tet2 KO mice. JAK2V617F KI/IP-10 KO (JAK IP-10) mutant mice were obtained by crossing JAK2V617F KI mice with IP-10 KO mice. To generate the triple-mutant allelic series (JAK TET IP-10), JAK2V617 KI/IP-10 KO mice were crossed with Tet2 KO mice. All procedures were performed under project licenses PPL 70/8406 and PEAD116C1, in compliance with the guidance on the operation of Animals Scientific Procedures Act (ASPA) 1986, following ethical review by the individual University of Cambridge or University of York Animal Welfare and Ethical Review Body (AWERB).

Mouse Serum Cytokine Profiling

PB samples (∼150 μL) were collected from the tail vein of WT mice, TET mice, JAK2 mice, combinatorial JAK TET mice, and CALR Del52 (CALR), aged 16 weeks, or by cardiac puncture for homozygous JAK2V617F KI mice, due to phenotype reducing the amount of serum obtained per mL of blood. Samples were left undisturbed at room temperature for 30 minutes. The clot was removed by centrifuging the samples at 2,000 $\times$ *g* for 10 minutes in a refrigerated centrifuge. The resulting supernatant (serum) was transferred into clean polypropylene tubes and subsequently stored at −20°C. Cytokine levels in mouse serum samples were assayed using the MILLIPLEX MAP Mouse Cytokine/Chemokine Magnetic Bead Panel (Millipore). The levels of 32 cytokines were quantified: eotaxin, granulocyte-macrophage colony−stimulating factor (GM-CSF), interleukin (IL)-1α, IL-2, IL-4, IL-6, IL-9, IL-12 (p40), IL-13, IL-17, vascular endothelial growth factor (VEGF), granulocyte colony−stimulating factor (G-CSF), IFN-γ, IL-1β, IL-3, IL-5, IL-7, IL-10, IL-12 (p70), IL-15, IP-10, regulated upon activation, normal T-cell expressed and secreted (RANTES), keratinocyte-derived chemokine (KC), lipopolysaccharide-induced CXC chemokine (LIX), macrophage colony−stimulating factor (M-CSF), macrophage inflammatory protein (MIP)-1α, MIP-2, TNF-α, leukemia inhibitor factor (LIF), MCP-1, monokine induced by IFN-γ (MIG), and MIP-1β. The plate was run on a Luminex xMAP machine to detect mean fluorescence intensity (MFI) values for each analyte-specific bead set. Cytokine concentrations were determined by xPONENT software (Luminex) based on the fit of a standard curve for MFI versus pg/mL. The values used were derived from the known reference concentrations supplied by the manufacturer. All cytokines ranged within the quality control values. Raw cell values were exported from Magpix xMAP exponent software into Microsoft Excel with pg/mL values calculated on the basis of the standard curves automatically generated.

Analysis of PB Samples from WT, JAK, TET, IP-10, Double- and Triple-crosses

PB samples were collected in EDTA-coated microvette tubes (Sarstedt AGF & Co., Nuembrecht, Germany). Blood was collected from the tail vein of 16-week-old mice. PB cell counts were performed using a Woodley ABC blood counter (Woodley Equipment, Bolton, UK) or a Vet ABC blood counter.

Isolation of human hematopoietic stem and progenitor cells (human HSPCs)

Fresh PB samples (40−60 mL, collected in Lithium-Heparin tubes) or frozen viable mononuclear cells (MNCs) were obtained from the patient's PB or BM. MNCs were isolated by density gradient centrifugation (Lymphoprep; Axis-Shield, Oslo, Norway) and enriched for CD34-positive cells (EasySep Human CD34+ enrichment kit, STEMCELL Technologies, Vancouver, Canada [STEMCELL]) as per the manufacturer's guidelines, except that only one round of depletion in the magnet was performed. Cells were then stained with the following antibodies: CD38/fluorescein isothiocyanate (FITC) (Clone HIT2, BD Biosciences, San Jose, CA, US), CD34/PerCPCy5.5 (Clone

581, BioLegend, San Diego, US), CD10/APC-Cy7 (Clone HI10a, BioLegend), CD90/APC (Clone 5E 10, BioLegend or BD), CD45RA/Violet450 (Clone HI1100, BD), and CD135/PE (Clone BV10A4H2, BioLegend). Single $CD34^+CD38^-CD90^+CD45RA^-$ cells (hereafter "hematopoietic stem cells (HSCs)" [27] were isolated for liquid culture using an Influx sorter (BD), equipped with the following lasers: 405 nm, 488 nm, 561 nm, and 640 nm, and filter sets; 530/40 (for FITC), 710/50 (for peridinin chlorophyll protein-Cyanine5 [5PerCPcy5.5]), 750LP (for allophycocyanin-Cyanin7 [APC-Cy7], 670/30 (for allophycocyanin [APC]), 460/50 (for Violet450), and 585/29 (for phycoerythrin [PE]).

Liquid cultures and clone size determination of human long-term repopulating HSCs (LT-HSCs)

Single HSCs from patient PB were sorted into 96-well plates and cultured in StemSpan (STEMCELL), cc100 cytokine cocktail (STEMCELL), Penicillin/Streptomycin (Sigma-Aldrich, St. Louis, MO), L-glutamine (Sigma-Aldrich), and 2-mercaptoethanol (Life Technologies, Carlsbad, CA)—with ["treated"] or without ["untreated"] IP-10 [50 or 100 ng/mL]. Cells were cultured at 37°C with 5% CO_2. Clone survival (≥2 cells/well) and proliferation were assessed after 7−10 days of culture. A minimum of eight clones were present in all untreated controls.

Isolation of the mouse E-SLAM HSCs

BM cells were isolated from the spine, sternum, femora, tibiae, and pelvic bones of both hind legs of WT mice by crushing the bones in 2% fetal calf serum (FCS, STEMCELL, or Sigma-Aldrich) in phosphate−buffered saline (PBS, Sigma-Aldrich). Red cell lysis was performed by treatment with ammonium chloride (NH_4Cl, STEMCELL). Depletion of mature lineage cells was performed using the EasySep mouse hematopoietic progenitor cell enrichment kit (STEMCELL). HSCs were isolated from the lineage depleted cell suspension using fluorescence-activated cell sorting using $CD45^+EPCR^+CD48^-CD150^+Sca-1^{high}$ (E-SLAM Sca-1^{high}) as described previously [28], using CD45 FITC (clone 30-F1,1 BD Biosciences), EPCR PE (clone RMEPCR1560, STEMCELL), CD150 PE-Cy7 (clone TC15-12F12.2, both from BioLegend), CD48 APC (clone HM48-1, BioLegend), Sca-1 Brilliant Violet (BV) 421 (clone D7, BioLegend), and 7- amino actinomycin D (7AAD) (Life Technologies). The cells were sorted in either purity or single sort mode on an Influx cell sorter (BD Biosciences) using the following filter sets: 488 530/40 (for FITC), 561 585/29 (for PE), 405 460/50 (for BV421), 640 670/30 (for APC), 561 750LP (for PE/Cy7), 640 750LP (for APC/Cy7), 405 520/35 (for BV510), and 561 670/30 (for 7AAD). When single HSCs were required, the single-cell deposition unit of the sorter was used to deposit one cell into each well of a round bottom 96-well plate, each well having been preloaded with 50−100 μL of medium.

Liquid culture and clone size determination of mouse HSCs

Single HSCs were sorted into 96-well U-bottom plates (Corning) and cultured in 100 μL StemSpan SFEM (STEMCELL) supplemented with 100 units/mL penicillin. and 100 μg/mL streptomycin (Pen/Strep, Sigma-Aldrich), 2 mmol/l L-glutamine (Sigma-Aldrich), 10^{-4} M 2-mercaptoethanol (Sigma-Aldrich), and 20 ng/mL IL-11 (Biotechne,

Abingdon, UK), and 300 ng/mL stem cell factor (SCF, R&D). A 50 ng/mL IP-10 (Miltenyi Biotec, Auburn, CA) was supplemented when specified. Cells were cultured at 37°C, 5% CO_2. Cell counts were performed daily every 22−24 hours, and cell cycle kinetics were determined for the first and second divisions using visual inspection, manually scoring each well as having 1, 2, or 3−4 cells. Cell survival was assessed using visual inspection on day 10 (the sorting day is determined as day 0), and clones were scored as very small (VS, less than 50 cells), small (S, 50−500 cells), medium (M, 501−5,000 cells), large (L, 5,001−10,000), and extra-large (XL, 10,001 or more cells).

Intracellular cytokine detection in human PB mononuclear cells (PBMCs).

Patient PB mononuclear cells (PBMNCs) were isolated as described above. A total of 2−5 × 10^6 cells/well were plated in 1 mL of RPMI (Sigma-Aldrich) 10% fetal calf serum (FCS) in a 12-well plate. For cytokine stimulations, IFN-γ was used at a final concentration of 5,000 U/mL (Miltenyi Biotec). Secretion inhibitor (BD Golgi-STOP, BD Biosciences) was added to both unstimulated and stimulated conditions (0.6 μL/well). Cells were incubated at 37°C for 4 hours (phorbol myristate acetate [PMA]/Ionomycin, or lipopolysaccharide [LPS] stimulation). After stimulation, MNCs cells were washed twice in PBS, treated with Fc receptor blocking (BD Biosciences), and then stained for cell surface markers: CD45/V450 (HI30, BD Biosciences), CD3/AF700, CD14/PE-Cy7 (M5E2, BD Biosciences or BioLegend), CD15/BV605 (W6D3, BD Biosciences), and CD56/BV711 (NCAM16.2, BD Biosciences), CD19/APC-Cy7 (SJ25-C1, Life Technologies). Zombie Aqua (BioLegend) was added in some experiments. Cells were incubated at 4°C for 30 minutes, then washed with staining buffer (PBS, 2% FCS). Cells were resuspended in fixation/permeabilization solution (BD, 200 μL/tubes or 100 μL/well) for 20 minutes at 4°C, washed twice with 250 μL/well 1 × BD Perm/Wash buffer, and resuspended in staining buffer. Stained and fixed cells were kept at 4°C for up to 12 hours before proceeding with intracellular cytokine staining. Fixed/permeabilized cells were resuspended in BD Perm/Wash buffer containing a conjugated anticytokine antibody. Cells were stained for 30 minutes at 4°C with anti-IP-10/PE (6D4/D6/G2, BD Biosciences). Samples were washed, resuspended in a staining buffer, run on a BD Fortessa flow cytometer, and analyzed in FlowJo10. The different cell populations were defined as follows: $CD56^-CD3^+$ (T cells), $CD3^-CD56^+$ (NK cells), $CD3^+CD56^+$ (NK T cells), $CD15^+CD14^-$ (granulocytes), $CD14^+CD56^-$ ($CD14^{+CD56^-}$ monocytes), $CD14^+CD56^+$ ($CD14^+CD56^+$ monocytes), and $CD34^+$ (progenitors) (Supplementary Figure E1).

Transplantation of JAK TET Double-Mutant HSCs into IP-10 Recipients

Donor cells were obtained from JAK TET mice. Competitor cells (3 × 10^5 whole BM cells from IP-10 KO mice) were transplanted alongside the donor cells (25 JAK TET HSCs/recipient). Recipients were WT, purchased from Charles River Laboratories (Saffron Walden, Essex, UK), or IP-10 mice purchased by The Jackson Laboratory, irradiated with two doses (2 × 550 Gy, separated by > 4 hours) using Caesium irradiation, and transplants were performed by intravenous tail vein injection using a 29.5-G insulin syringe.

Flow Cytometric Analysis of BM and Spleen from WT, JAK, TET, IP-10, Double- and Triple-Crosses

BM and spleen tissues were collected from 16-week-old mice. As above, BM was processed using flushing iliac bones, tibiae, and femurs with 2% FCS in PBS. The spleen was processed by gently cutting it into small pieces and then pressed through a 70-micron cell strainer with a 1-mL syringe plunger (Greiner Bio-One Ltd.). Samples were stained with the following antibodies: CD71/FITC (Clone R17217, Cat no. 113806), TER119/PE-Cy7 (Clone TER-119, Cat no. 116221), CD3/PE (Clone 17A2, Cat no. 100206), B220/APC (Clone RA3-6B2, Cat no. 103212), Ly6G/BV421 (Clone 1A8, Cat no. 127628), and CD11b/BV785 (Clone M1/70, Cat no. 101243). All antibodies were obtained from BioLegend. To obtain single-cell suspensions, all samples were filtered through a 70-μm cell strainer and treated with 7-amino actinomycin D (7AAD, Invitrogen) for live/dead cell discrimination. After gating for viable cells, the different stages of erythroblast differentiation (I through V) were defined based on CD71/Ter-119 expression Supplementary Figure E2 The precise borders between these regions were determined arbitrarily [29]. All data were acquired on an LSD Fortessa X-20 (BD Biosciences) instrument and were analyzed using FlowJo v10.9.0 (FLOWJO LLC, Ashland, OR).

RESULTS

Serum IP-10 Levels are Associated with *JAK2* and *TET2* Mutations in Patients with MPN

Previously, we undertook a PB serum screen of 38 cytokines across a wide range of phenotypic human MPN disease subtypes [10]. For most cytokines, no differences across patients were observed based on mutational status alone, suggesting that a single genetic lesion or combination of lesions does not dominantly instruct microenvironmental heterogeneity. One molecule (IP-10), however, was positively correlated with the JAK2V617F variant allele fraction (VAF) in patients with MPN (Figure 1a). When additional mutations were considered in combination with JAK2V617F, patients who carried mutations in epigenetic regulators (*TET2, DNMT3A, ASXL1, EZH2,* or *IDH1/2*) in combination with JAK Hom had the highest levels of IP-10 in both polycythemia vera (PV) and myelofibrosis (MF) subtypes when compared with patients carrying *JAK2*-heterozygous (JAK Het), *CALR,* or *MPL* mutations (Neg) (Figure 1b), suggesting that larger and more advanced MPN clones might produce more IP-10. Moreover, patients homozygous for the JAK2V617F mutation who also had a loss-of-function mutation in *TET2,* the gene most commonly commutated with *JAK2,* had the highest IP-10 concentration, and this was irrespective of disease subtype (Figure 1c).

We next set out to determine whether IP-10 levels were similarly dysregulated in a wide range of MPN mouse models where driver mutations are present. IP-10 levels were highest in *Tet2*$^{-/-}$ mice (TET) and combinatorial *Jak2*$^{V617F/V617F}$*Tet2*$^{-/- \ or \ +/-}$ (JAK Hom TET) compared with both WT and CALR^{del52} mice [24], mirroring the findings in patient samples (Figure 1d). This shared overproduction of IP-10 across both mice and humans suggests that its dysregulation is linked to mutations in *JAK2* and *TET2* and situates these mouse models as powerful tools to study the effect of IP-10 on disease establishment and/or progression.

A Broader Range of Cells Produce IP-10 in More Advanced MPNs

To further examine different disease-specific microenvironments, we surveyed the mature blood cell types making IP-10. We profiled IP-10 production in patient PBMNCs by flow cytometry, including mature cell markers (T cells, NK cells, monocytes, and granulocytes) [10] (Supplementary Figure E1). In bulk leukocytes without stimulation, IP-10 production was detected in five out of 15 patient samples (> 3% positive cells of total PBMNCs) and these five patients had either PV or MF. Upon IFN-γ stimulation, production of IP-10 increased in the majority of patients as well as healthy controls with the highest IP-10 production once again associated with more advanced stages of disease (Figure 2a). In agreement with previous studies [30], monocytes were the predominant producer of IP-10 across all samples, but a population of IP-10-positive CD14$^+$CD56$^+$ pro-inflammatory monocytes was observed in some patients with MPN (Figure 2b and c), and these latter cells were particularly high in PV4, whose JAK2V617F mutant allele burden was >95% in granulocytes (Figure 2c). There was also increased production of IP-10 by T cells in 3 of 5 patients with MF (Figure 2b and c), further supporting the production of IP-10 by a wider range of cells compared with normal controls and patients with essential thrombocythemia (ET). Interestingly, IP-10 production by PBMNCs in vitro strongly correlated with the IP-10 concentration measured in serum (n = 14 patients, r = 0.82, Figure 2d), but IP-10 did not have a direct effect in vitro on single HSCs (Supplementary Figure E3). Together, these results indicate that CD14$^+$ monocytes are the main producers of IP-10. Subsets of monocytes and T cells might feature as components of a distinct MPN microenvironment observed in more severe disease subtypes; however, further evidence in a larger cohort of patients is necessary to substantiate this observation.

Microenvironmental Loss of IP-10 Does not Prevent JAK2-TET2- Double-Mutant HSCs From Driving Disease

Although treatment with IP-10 did not directly affect mutant HSC survival in vitro, its role in the context of the in vivo microenvironment remains unclear. We therefore generated an in vivo model to determine the role of IP-10 in the context of MPN initiation and evolution. IP-10-deficient mice do not have a severe phenotype on their own but do show impaired T-cell function, including a defect in T-cell proliferation and recruitment of effector T cells in response to specific antigenic challenges, such as stimulation with ovalbumin [20]. To investigate whether the absence of IP-10 affects HSC function in vitro, single E-SLAM Sca-1^{high} HSCs [25] were isolated from WT and IP-10 KO mice and cultured in vitro for 10 days, tracking divisional kinetics and clone survival as described previously [21]. The time to first, second, and third division of IP-10 KO HSCs overlapped nearly identically with WT HSCs (Supplementary Figure E4a). Clone survival and clonal proliferation over the 10-day culture were also highly similar to those of WT mice, as measured by assessing clone size distribution, suggesting that there were no major perturbations of HSC function in vitro due to the absence of IP-10 alone (Supplementary Figure E4b and c).

To investigate whether a robust disease could be established and maintained in an IP-10-deficient environment, we transplanted JAK2 TET2 double-mutant HSCs [21] into either WT or IP-10 deficient recipients. A total of 100 CD45$^+$EPCR$^+$CD150$^+$CD48$^-$ LT-HSCs
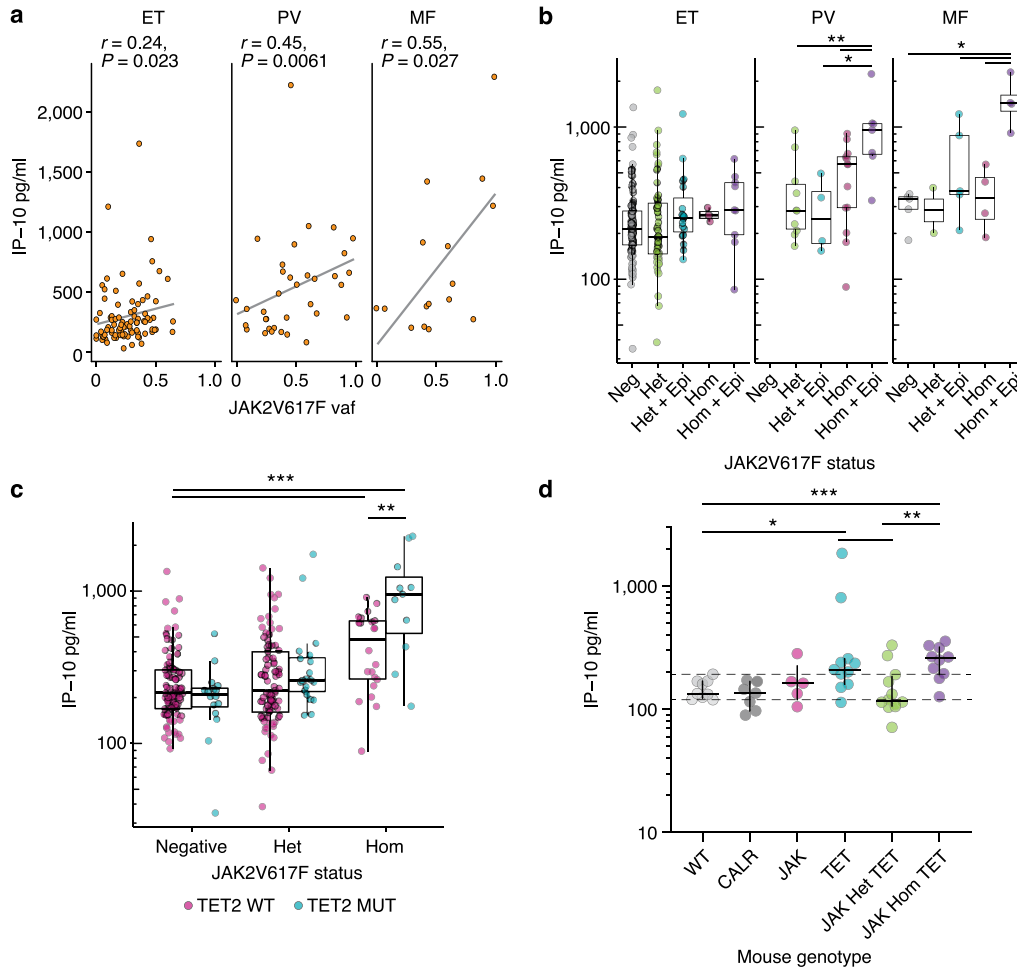
Figure 1 Serum levels of interferon gamma (IFN-γ)−induced protein-10 (IP-10) correlate with JAK2 and TET2 mutational status. **(A)** Correlation of IP-10 serum levels with JAK2V617F burden in each disease subtype. High levels of IP-10 correlate with an increase in JAK2V617F allele burden. **(B)** Serum IP-10 levels in patients with essential thrombocythemia (ET), polycythemia vera (PV), and myelofibrosis (MF) (JAK2-mutation negative [Neg], gray circles; JAK2V617F heterozygous alone [Het], green circles; JAK2Het with an additional epigenetic mutation [Het + Epi], blue circles; JAK2V617F homozygous alone [Hom], pink circles; and JAK2Hom with an additional epigenetic mutation [Hom + Epi], purple circles). Patients with JAK Hom + Epi reported the highest levels of IP-10 in both the PV and MF subgroups. **(C)** IP-10 serum levels in patients with *JAK2* and *TET2* mutations. Patients with JAK2V617F-positive (Hom) have increased levels of IP-10 compared with nonmutant patients (Negative). The highest levels of IP-10 are detected in patients with both JAK2 homozygosity (Hom) and *TET2* mutations (TET2 MUT). Bars show medians with interquartile range (IQR). Mann-Whitney U test *$p < 0.05$, **$p < 0.01$, ***$p < 0.001$, ****$p < 0.0001$. **(D)** IP-10 levels in mouse models of myeloproliferative neoplasms. Serum levels of IP-10 in wild-type (WT, n = 9), CALRdel5 (CALR, n = 7), JAK2V617F KI Hom (JAK, n = 5), TET2 KO (TET, n = 11), JAK Het TET (n = 12), and JAK Hom TET (n = 19) mice. Serum levels of IP-10 are increased in TET and JAK Hom TET mice, compared with WT control mice. Bars show a median with IQR. Mann-Whitney U test: * $p < 0.05$, **$p < 0.01$, ***$p < 0.001$.

(E-SLAM, ∼50% functional HSCs by single-cell transplantation [25,28]) were isolated from JAK TET mice, and 25 cells/mice were transplanted alongside IP-10 KO helper cells (300,000 cells/mouse) into WT or IP-10 KO recipient mice. Recipients were serially bled at 4-, 8-, 12-, 16-, and 20-weeks post-transplantation and PB cell counts were performed to monitor hematocrit (HCT) levels, hemoglobin (Hb) levels, platelet (Plt) counts, and white blood cell (WBC) counts (Figure 3a). Both WT and IP-10 KO recipients showed an increase in HCT and Hb levels, resembling the donor PV-like phenotype, and demonstrated that the absence of host-derived IP-10 does not

prevent JAK TET HSCs from initiating an MPN in a transplantation setting. IP-10 KO and WT recipients show comparable Plt counts at all time points. At 12 weeks post-transplantation, a slight increase in HCT levels and WBC counts were observed in IP-10 KO mice compared with the WT recipients, and WT recipients showed higher Hb levels at week 8 post-transplantation (Figure 3b).

Together, these results indicate that the removal of IP-10 from the host microenvironment does not prevent the initiation of disease when JAK TET HSCs are transplanted into IP-10 KO mice. This could be due to the mutant donor cells creating their own IP-10 as the
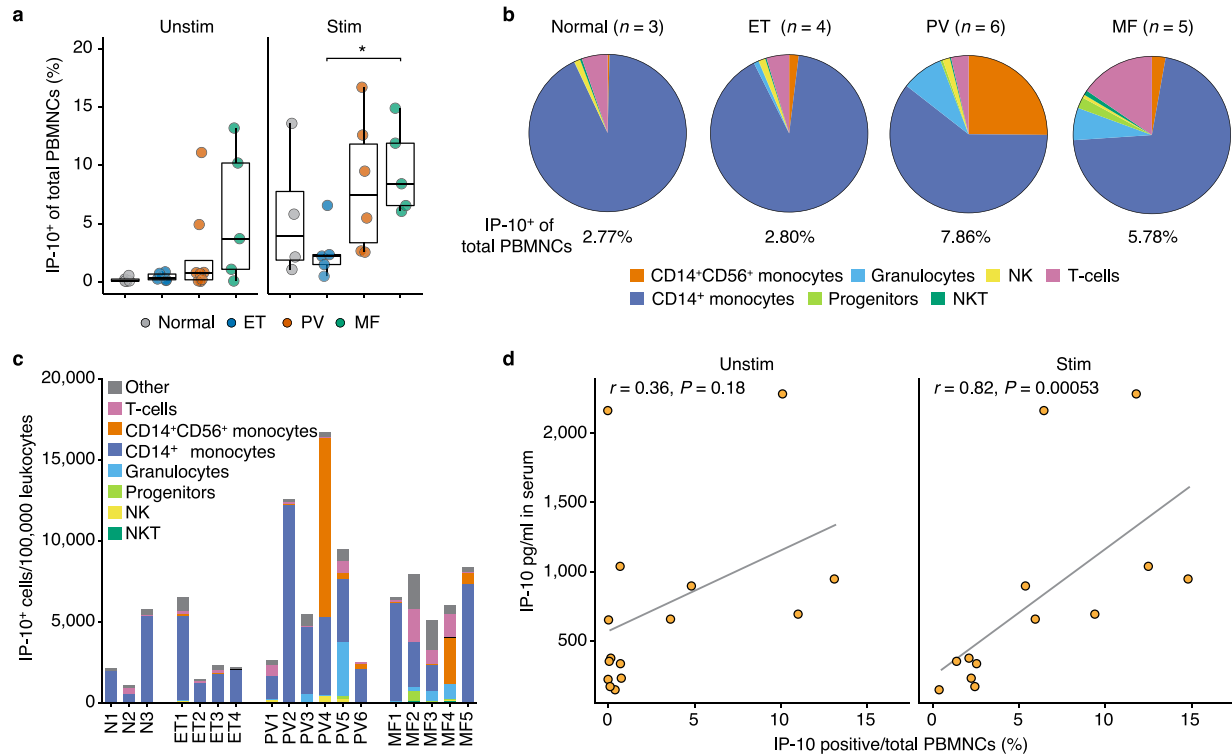
Figure 2 Aberrant production of interferon gamma (IFN-γ)-induced protein-10 (IP-10) from CD14$^+$CD56$^+$ pro-inflammatory monocytes and T cells from patients with myeloproliferative neoplasm (MPN). **(A)** Peripheral blood mononuclear cells (PBMNCs) from patients with MPN (17 of 18 carrying JAK2 mutations, one with a CALR mutation) were stimulated with interferon gamma (IFN-γ) for 4 hours and profiled using flow cytometry. IFN-γ-induced protein-10 (IP-10) levels are higher in patients with polycythemia vera (PV) and myelofibrosis (MF) compared with patients with essential thrombocythemia (ET). **(B)** The distribution of cell types producing each cytokine post-stimulation is displayed in individual pie charts by disease subtype. IP-10 is mainly produced by monocytes. The percentages displayed underneath each pie chart are the median percentage of positive cells out of total CD34 mononuclear cells (MNCs). **(C)** Cell types producing IP-10, are shown for individual patients (n = 4 ET, n = 6 PV, and n = 5 MF). **(D)** Correlation of IP-10 (in both stimulated and unstimulated PBMNCs) with the original IP-10 concentration measured in serum (n = 14).

clone grows, which may help maintain the disease. The mild reduction in HCT and Hb levels in the early stages of the purified JAK TET HSC transplantation experiments accords with this possibility, where HSCs would not be expected to have generated large numbers of mature IP-10-secreting cells at early time points.

Combinatorial loss of IP-10 with JAK2V617F and TET2 loss-of-function mutations partially ameliorates the PV-like phenotype

To exclude the possibility that transplantation of donor JAK TET HSCs (and/or their progeny) leads to the re-introduction of IP-10 into the environment, we pursued genetic approaches to assess the effects of the complete absence of IP-10 on disease biology. The first approach consisted of crossing IP-10 KO mice with the JAK2V617F KI line to generate a model that would completely deplete IP-10 from a JAK2-mutant background. PB was collected and analyzed from 16-week-old JAK IP-10 double-mutant mice. A mild decrease in Hb levels was observed in JAK IP-10 mice (both IP-10 Het and IP-10 KO) compared with the JAK Hom mice (Figure 4 and Supplementary Figure E5), suggesting that loss of IP-10 might partially ameliorate the phenotype; however, HCT levels were still high in both settings.

Since IP-10 expression levels were higher in the presence of a TET2 homozygous mutation in both patients and mice, our next approach was to cross the JAK IP-10 double-mutant mice with TET2 KO mice to generate a triple-mutant mouse model (JAK2$^{V617F/V617F}$TET2$^{-/-}$IP-10$^{-/-}$, or "JAK TET IP-10"). Serial disease monitoring of various genotypes—both single and triple-mutants—revealed that only JAK2 homozygous mice (JAK Hom) displayed a strong red blood cell phenotype when mutated as a single allele. In a similar fashion to WT mice, TET IP-10 double KO mice (TET Hom IP-10 Hom) did not develop a red cell phenotype. The triple-mutant mice (JAK Hom TET Hom IP-10 Hom), however, displayed a partial amelioration of disease, whereby triple-mutant mice had reduced HCT and Hb counts compared with JAK2 homozygous mice (JAK Hom) and JAK IP-10 double-mutant mice (JAK Hom IP-10 Hom) (Figure 4). The phenotype resolution we observe is highly unlikely to be attributable to the absence of TET2 on a JAK-mutated background since previous work has shown that JAK2 TET2 double-mutant mice have a more severe red cell phenotype than mice carrying a JAK2 mutation alone [21].

In contrast, the reduction in red cells was not observed in the JAK Hom IP-10 Hom or JAK TET Het IP-10 mice (JAK Hom TET Het IP-10 Hom) (Supplementary Figure E5), suggesting that complete loss of
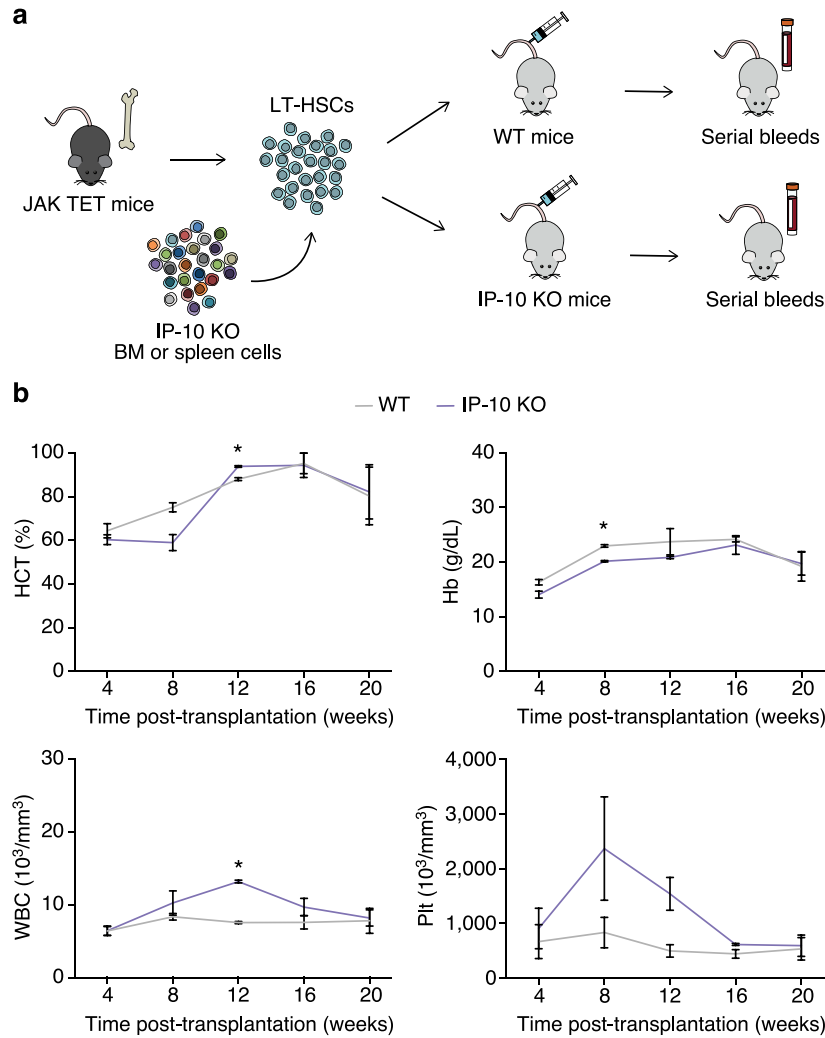
Figure 3 Interferon gamma (IFN-γ)-induced protein-10 (IP-10) is not required for the development of the disease in a murine transplantation model of myeloproliferative neoplasms (MPN). **(A)** Transplantation of JAK TET cells into IP-10 knockout (KO) or wild-type (WT) recipients. Bulk LT-HSCs (25 per mouse) were sorted from JAK TET (JAK2V617F KI/TET2KO) mutant mice and transplanted into either WT (n = 2) or IP-10 KO (n = 2) recipients, along with bone marrow (BM) cells from IP-10 KO ("helper cells," 300,000 per mouse). Serial bleeds were taken at 4-, 8-, 12-, 16-, and 20-weeks post-transplantation and peripheral blood cell parameters were analyzed. **(B)** Hematocrit (HCT) levels, hemoglobin (Hb) levels, white blood cell (WBC) counts, and platelet (Plt) counts for IP-10 KO and WT recipients transplanted with the same donor cells. No significant differences were observed in Plt counts at any time point. A slight increase in HCT and WBC is reported in IP-10 KO mice compared with WT recipients (p = 0.0186 and p = 0.002, respectively) at week 12 post-transplantation, and in Hb levels in WT mice compared with IP-10 KO at week 8 post-transplantation (p = 0.0103). Bars show the mean with the standard error of the mean (±SEM). Unpaired t-test: *p < 0.05, **p < 0.01, ***p < 0.001, ****p < 0.0001.

TET2 activity creates a dependency on IP-10 driven biology in a JAK2 homozygous background. No statistically significant differences in WBC and Plt counts were observed across the cohort.

The Absence of IP-10 Reduces the Impact of JAK2 V617F on Erythroid Differentiation

As previously reported by Li et al. [23], the JAK2-mutant mice (JAK Hom) present a PV-like phenotype, displaying a marked increase in HCT, expansion of erythroid cells, and splenomegaly. To investigate whether the cellular composition of red cell progenitors was altered by the absence of IP-10 and/or TET2 on a JAK2V617F mutant background, BM and spleen cells from 16-week-old mutant mice were isolated and analyzed for mature/progenitor cell composition using flow cytometry. In the BM, JAK Hom mice have reduced pro-erythroblasts and increased terminally differentiated CD71⁻Ter119⁺ cells. In accordance with the amelioration of HCT and Hb values in the PB described above, the triple-mutant mice show a reversal of these phenotypes, with restored levels of pro-erythroblasts and terminally differentiated CD71⁻Ter119⁺ cells. Interestingly, TET2 mutant mice
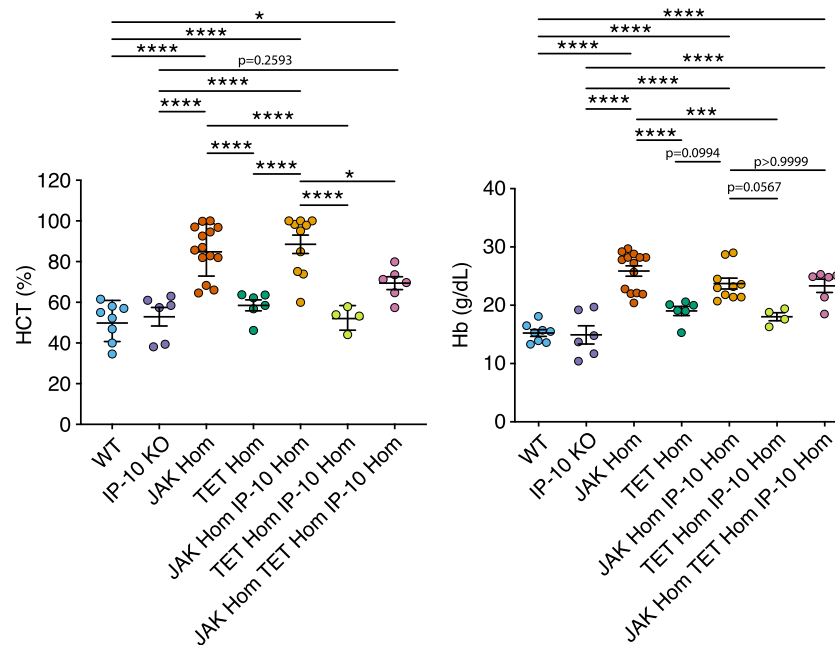
Figure 4 Interferon gamma (IFN-γ)-induced protein-10 (IP-10) loss results in a modest reduction in hematocrit (HCT) levels in JAK homozygous (Hom) TET Hom IP-10 Hom mice compared with JAK Hom and JAK Hom IP-10 Hom mice. Sixteen-week-old mice (n = 8 wild-type [WT], n = 6 IP-10 knockout [KO], n= 14 JAK Hom, n = 6 TET Hom, n = 10 JAK Hom IP-10 Hom, n = 4 TET Hom IP-10 Hom, and n = 6 JAK Hom TET Hom IP-10 Hom) were bled, and blood cell counts were performed. The graphs show hematocrit (HCT) and hemoglobin (Hb) levels. JAK Hom, JAK Hom IP-10 Hom. and JAK Hom TET Hom IP-10 Hom mice showed increased HCT and Hb levels compared with WT mice. A slight reduction in HCT levels was observed in JAK Hom TET Hom IP-10 Hom mice compared with JAK Hom IP-10 Hom ($p < 0.05$) and JAK Hom ($p < 0.05$) mice. One-way analysis of variance (ANOVA) (Tukey's multiple comparisons test): *$p < 0.05$, **$p < 0.01$, ***$p < 0.001$, ****$p < 0.0001$. Bars show the mean with the standard error of the mean (±SEM).

were observed to have a depletion of terminally differentiated CD71⁻Ter119⁺ cells, which may initiate a selective evolutionary pressure to acquire JAK2 V617F mutations (Figure 5).

Spleen size was measured at experimental endpoints, and although triple-mutant mice showed an elevated spleen size compared with WT mice, they were not increased in size compared with JAK2 homozygous mice (JAK Hom) (Supplementary Figure E6).

Together, these data show that the concomitant loss of TET2 and IP10 on a JAK2V617F mutant background results in a less intense MPN phenotype with respect to both red cell progenitors and overall red cell phenotypes, thereby implicating IP-10 as a potential regulator of advanced-stage MPNs.

DISCUSSION

A number of recent studies have drawn attention to the BM microenvironment as a driver of clonal selection in heterogeneous populations of normal and malignant blood stem cell clones [31]. Within this body of work, multiple studies have implicated interferon signaling in both HSC function [32−34] and MPN biology [35−37], and it continues to be one of the leading candidate regulators of disease-driving HSCs. In this study, we identify a role for IP-10 in MPN biology, whereby higher levels of IP-10 strongly correlate with increasing disease severity and the presence of both *JAK2* and *TET2* mutations. Using a series of MPN mouse models, we show the same correlation

with advanced disease, whereby JAK2 TET2 double-mutant mice had the highest levels of IP-10. This allowed us to undertake further studies to investigate its role in various hematopoietic lineages and in the alteration of red cell production. Together, our data suggest that IP-10 might be usefully explored as a potential therapeutic target for ameliorating the impact of the MPN clone.

Our in vitro data using both human and mouse-purified HSCs show that IP-10 does not act directly on the core disease-driving aspects of HSC biology: increased HSC proliferation and survival. This, in addition to the lack of IP-10 receptor (CXCR3) expression on HSCs [38], suggests that IP-10 acts on cells downstream of the HSC and is involved in modulating the disease phenotype rather than the seed cells of the disease itself. However, it is also formally possible, as has been previously reported for other cytokines [33,39−42], that the effect of IP-10 on HSCs might be different in vivo, but this would require extensive future work.

Curiously, the disease-ameliorating effect of IP-10 loss was only observed in combination with TET2 loss of function, the latter of which typically makes the MPN phenotype worse [43,44], not better. The presence of higher IP-10 levels in patients with JAK2 mutants with *TET2* commutations further supports the existence of a functional link between TET2 and IP-10, especially since the loss of IP-10 in the JAK2 model without *TET2* mutations had only very modest effects on improving disease phenotype. As TET2 is a global regulator of deoxyribonucleic acid (DNA) methylation patterns, it is possible that its loss might also contribute to the dysregulation of genes that
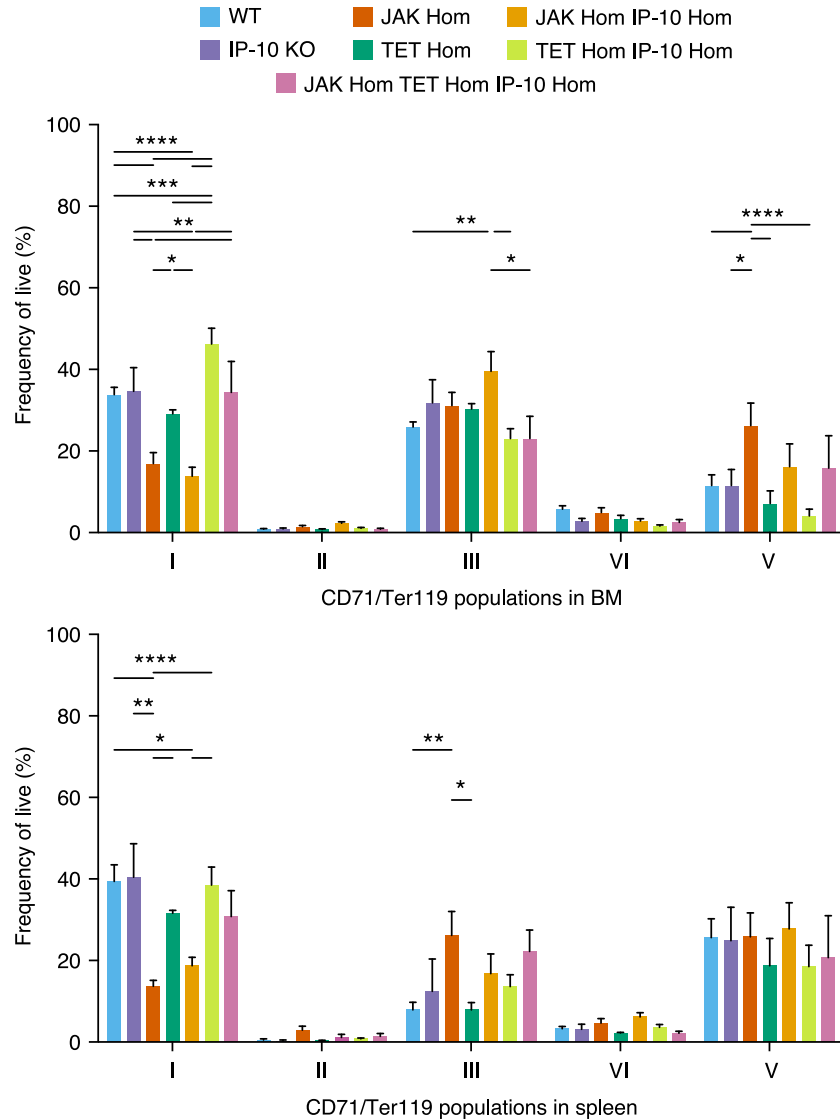
Figure 5 The increase in frequency of CD71⁻Ter-119⁺ terminally differentiated erythroblasts observed in JAK homozygous (Hom) mice compared with wild-type (WT) mice is attenuated in JAK Hom TET Hom interferon gamma (IFN-γ)-induced protein-10 (IP-10) Hom mice. Bone marrow (BM) and spleen cells from 16-week-old mice (n = 17 WT, n = 4 IP-10 knockout (KO), n = 7 JAK Hom, n = 6 TET Hom, n = 5 JAK Hom IP-10 Hom, n = 7 TET Hom IP-10 Hom, and n = 4 JAK Hom TET Hom IP-10 Hom) were isolated and differentiated cell composition analyzed. Representative fluorescence-activated cell sorter (FACS) profiles showing cells stained with CD71 and Ter119 antibodies are shown in Supplementary Figure E2; I through V correspond to progressive stages of erythroid differentiation. An increase in stage V terminally differentiated erythroblasts (CD71⁻Ter119⁺) is observed in the BM and spleen of JAK Hom mice compared with WT mice. A slight decrease in stage V BM erythroblasts is observed in the BM and spleen of JAK Hom TET Hom IP-10 Hom compared with JAK Hom mice. JAK Hom mice show a decrease in stage I BM and spleen erythroblast (CD71⁻Ter119⁻) compared with WT mice, even a higher decrease in the BM of JAK Hom IP-10 Hom mice compared with WT mice, and the frequency is mildly restored in BM and spleen from JAK Hom TET Hom IP-10 Hom mice, with a frequency comparable to WT. Two-way analysis of variance (ANOVA) (Tukey's multiple comparisons test).

interact with or are regulated by, IP-10, further complicating the picture for understanding the mechanism by which only the triple-mutant mice show any phenotype resolution. Moreover, recent data have shown that the complete TET2 KO has a different impact on the hematopoietic system when compared with the catalytic-deficient TET2 KO that we used in this study, and this may also contribute to unique IP-10-related biology [45].

Recent studies have shown that the cytokine environment in MPN patients and/or MPN cell lines manifests pronounced regulatory patterns of certain factors, including IP-10, compared with healthy controls [46,47]. Moreover, such dysregulation in cytokine levels could potentially contribute to therapeutic resistance in MPN clones [47]. In general, altered cytokine levels such as IP-10 in patients with MPN might derive from hematopoietic (clonal and/or non-clonal) or

nonhematopoietic cell sources. One possible route would be the clonal expansion of mutated megakaryocytes or monocytes, whereby an increased cell number might translate into higher levels of specific cytokines, potentially driving increased angiogenesis or fibroblast differentiation/recruitment with consequent BM fibrosis [48,49]. However, it remains unclear whether an increase in monocyte number alone could explain the IP-10 levels or whether the novel T-cell source of IP-10 we observe in some patients might come into play. Either way, further investigation of potential targets of IP-10 and its cellular source will be required to clarify the exact effect of this cytokine on the microenvironment and its potential role in disease pathogenesis or targetability for therapy.

Conflict of Interest Disclosure

The authors do not have any conflicts of interest to declare in relation to this work.

Acknowledgments

Author Contributions

MB, NFO, and DGK conceived and designed the experiments; MB, LCC, NFO, JL, JM, EB, MI, MSS, AHC, GB, LMR, JLCC, CAO, and JLB performed the experiments; MB, LCC, NFO, and JG analyzed the data; and MB, LCC, JLB, and DGK wrote the paper with input from ARG.

SUPPLEMENTARY MATERIALS

Supplementary material associated with this article can be found online at https://doi.org/10.1016/j.exphem.2024.104246

REFERENCES

1. Panteli KE, Hatzimichael EC, Bouranta PK, et al. Serum interleukin (IL)-1, IL-2, sIL-2Ra, IL-6 and thrombopoietin levels in patients with chronic myeloproliferative diseases. Br J Haematol 2005;130:709–15.
2. Tefferi A, Vaidya R, Caramazza D, Finke C, Lasho T, Pardanani A. Circulating interleukin (IL)-8, IL-2R, IL-12, and IL-15 levels are independently prognostic in primary myelofibrosis: a comprehensive cytokine profiling study. J Clin Oncol 2011;29:1356–63.
3. Boissinot M, Cleyrat C, Vilaine M, Jacques Y, Corre I, Hermouet S. Anti-inflammatory cytokines hepatocyte growth factor and interleukin-11 are over-expressed in polycythemia vera and contribute to the growth of clonal erythroblasts independently of JAK2V617F. Oncogene 2011;30:990–1001.
4. Kittang AO, Sand K, Brenner AK, Rye KP, Bruserud Ø. The systemic profile of soluble immune mediators in patients with myelodysplastic syndromes. Int J Mol Sci 2016;17:1080. 5.
5. Kornblau SM, McCue D, Singh N, Chen W, Estrov Z, Coombes KR. Recurrent expression signatures of cytokines and chemokines are present and are independently prognostic in acute myelogenous leukemia and myelodysplasia. Blood 2010;116:4251–61.
6. Sallman DA, List A. The central role of inflammatory signaling in the pathogenesis of myelodysplastic syndromes. Blood 2019;133:1039–48.
7. e Gonzalo-Calvo D, de Luxán-Delgado B, Martínez-Camblor P, et al. Chronic inflammation as predictor of 1-year hospitalization and mortality in elderly population. Eur J Clin Invest 2012;42:1037–46.
8. Hawkins ED, Duarte D, Akinduro O, et al. T-cell acute leukaemia exhibits dynamic interactions with bone marrow microenvironments. Nature 2016;538:518–22.
9. Kent DG, Green AR. Order matters: the order of somatic mutations influences cancer evolution. Cold Spring Harb Perspect Med 2017;7:a027060.
10. Øbro NF, Grinfeld J, Belmonte M, et al. Longitudinal cytokine profiling identifies GRO-α and EGF as potential biomarkers of disease progression in essential thrombocythemia. Hemasphere 2020;4:e371.
11. Fan W, Cao W, Shi J, et al. Contributions of bone marrow monocytes/macrophages in myeloproliferative neoplasms with JAK2^{V617F} mutation. Ann Hematol 2023;102:1745–59.
12. Massarenti L, Knudsen TA, Enevold C, et al. Interferon alpha-2 treatment reduces circulating neutrophil extracellular trap levels in myeloproliferative neoplasms. Br J Haematol 2023;202:318–27.
13. Gotfredsen K, Liisborg C, Skov V, Kjær L, Hasselbalch HC, Sørensen TL. Serum levels of IL-4, IL-13 and IL-33 in patients with age-related macular degeneration and myeloproliferative neoplasms. Sci Rep 2023;13:4077.
14. Li J, Malouf C, Miles LA, Willis MB, Pietras EM, King KY. Chronic inflammation can transform the fate of normal and mutant hematopoietic stem cells. Exp Hematol 2023;127:8–13.
15. Fleischman AG, Aichberger KJ, Luty SB, et al. TNFα facilitates clonal expansion of JAK2V617F positive cells in myeloproliferative neoplasms. Blood 2011;118:6392–8.
16. Bourantas KL, Hatzimichael EC, Makis AC, et al. Serum beta-2-microglobulin, TNF-alpha and interleukins in myeloproliferative disorders. Eur J Haematol 1999;63:19–25.
17. Hermouet S, Godard A, Pineau D, et al. Abnormal production of interleukin (IL)-11 and IL-8 in polycythaemia vera. Cytokine 2002;20:178–83.
18. Pourcelot E, Trocme C, Mondet J, Bailly S, Toussaint B, Mossuz P. Cytokine profiles in polycythemia vera and essential thrombocythemia patients: clinical implications. Exp Hematol 2014;42:360–8.
19. Madhurantakam S, Lee ZJ, Naqvi A, Prasad S. Importance of IP-10 as a biomarker of host immune response: critical perspective as a target for biosensing. Curr Res Biotechnol 2023;5:100130.
20. Dufour JH, Dziejman M, Liu MT, Leung JH, Lane TE, Luster AD. IFN-gamma-inducible protein 10 (IP-10; CXCL10)-deficient mice reveal a role for IP-10 in effector T cell generation and trafficking. J Immunol 2002;168:3195–204.
21. Shepherd MS, Li J, Wilson NK, et al. Single-cell approaches identify the molecular network driving malignant hematopoietic stem cell self-renewal. Blood 2018;132:791–803.
22. Harrison CN, Bareford D, Butt N, et al. Guideline for investigation and management of adults and children presenting with a thrombocytosis. Br J Haematol 2010;149:352–75.
23. Li J, Kent DG, Godfrey AL, et al. JAK2V617F homozygosity drives a phenotypic switch in myeloproliferative neoplasms, but is insufficient to sustain disease. Blood 2014;123:3139–51.

24. Li J, Prins D, Park HJ, et al. Mutant calreticulin knockin mice develop thrombocytosis and myelofibrosis without a stem cell self-renewal advantage. Blood 2018;131:649–61.

25. Wilson NK, Kent DG, Buettner F, et al. Combined Single-Cell Functional and Gene Expression Analysis Resolves Heterogeneity within Stem Cell Populations. Cell Stem Cell 2015;16:712–24.

26. Ko M, Bandukwala HS, An J, et al. Ten-eleven-translocation 2 (TET2) negatively regulates homeostasis and differentiation of hematopoietic stem cells in mice. Proc Natl Acad Sci U S A 2011;108:14566–71.

27. Doulatov S, Notta F, Eppert K, Nguyen LT, Ohashi PS, Dick JE. Revised map of the human progenitor hierarchy shows the origin of macrophages and dendritic cells in early lymphoid development. Nat Immunol 2010;11:585–93.

28. Kent DG, Copley MR, Benz C, et al. Prospective isolation and molecular characterization of hematopoietic stem cells with durable self-renewal potential. Blood 2009;113:6342–50.

29. Socolovsky M, Nam H, Fleming MD, Haase VH, Brugnara C, Lodish HF. Ineffective erythropoiesis in Stat5a(-/-)5b(-/-) mice due to decreased survival of early erythroblasts. Blood 2001;98:3261–73.

30. Lee EY, Lee ZH, Song YW. CXCL10 and autoimmune diseases. Autoimmun Rev 2009;8:379–783.

31. Leimkühler NB, Schneider RK. Inflammatory bone marrow microenvironment. Hematology Am Soc Hematol Educ Program 2019;2019:294–302.

32. Baldridge MT, King KY, Boles NC, Weksberg DC, Goodell MA. Quiescent haematopoietic stem cells are activated by IFN-gamma in response to chronic infection. Nature 2010;465:793–7.

33. Essers MA, Offner S, Blanco-Bose WE, et al. IFNalpha activates dormant haematopoietic stem cells in vivo. Nature 2009;458:904–8.

34. Trumpp A, Essers M, Wilson A. Awakening dormant haematopoietic stem cells. Nat Rev Immunol 2010;10:201–9.

35. Chen E, Beer PA, Godfrey AL, et al. Distinct clinical phenotypes associated with JAK2V617F reflect differential STAT1 signaling. Cancer Cell 2010;18:524–35.

36. Hasan S, Lacout C, Marty C, et al. JAK2V617F expression in mice amplifies early hematopoietic cells and gives them a competitive advantage that is hampered by IFNα. Blood 2013;122:1464–77.

37. Mullally A, Bruedigam C, Poveromo L, et al. Depletion of Jak2V617F myeloproliferative neoplasm-propagating stem cells by interferon-α in a murine model of polycythemia vera. Blood 2013;121:3692–702.

38. Groom JR, Luster AD. CXCR3 in T cell function. Exp Cell Res 2011;317:620–31.

39. Broxmeyer HE, Williams DE, Lu L, Cooper S, Anderson SL, Beyer GS, Hoffman R, Rubin BY. The suppressive influences of human tumor necrosis factors on bone marrow hematopoietic progenitor cells from normal donors and patients with leukemia: synergism of tumor necrosis factor and interferon-gamma. J Immunol 1986;136:4487–95.

40. Caux C, Saeland S, Favre C, Duvert V, Mannoni P, Banchereau J. Tumor necrosis factor-alpha strongly potentiates interleukin-3 and granulocyte-macrophage colony-stimulating factor-induced proliferation of human CD34+ hematopoietic progenitor cells. Blood 1990;75:2292–8.

41. Pearl-Yafe M, Mizrahi K, Stein J, et al. Tumor necrosis factor receptors support murine hematopoietic progenitor function in the early stages of engraftment. Stem Cells 2010;28:1270–80.

42. Pronk CJ, Veiby OP, Bryder D, Jacobsen SE. Tumor necrosis factor restricts hematopoietic stem cell activity in mice: involvement of two distinct receptors. J Exp Med 2011;208:1563–70.

43. Chen E, Schneider RK, Breyfogle LJ, Rosen EA, et al. Distinct effects of concomitant Jak2V617F expression and Tet2 loss in mice promote disease progression in myeloproliferative neoplasms. Blood 2015;125:327–35.

44. Kameda T, Shide K, Yamaji T, et al. Loss of TET2 has dual roles in murine myeloproliferative neoplasms: disease sustainer and disease accelerator. Blood 2015;125:304–15.

45. Flores JC, Ito K, Huang CY, et al. Comparative analysis of Tet2 catalytic-deficient and knockout bone marrow over time. Exp Hematol 2023;124:45–55.e2.

46. Schnöder TM, Eberhardt J, Koehler M, et al. Cell autonomous expression of CXCL-10 in JAK2V617F-mutated MPN. J Cancer Res Clin Oncol 2017;143:807–20.

47. Manshouri T, Estrov Z, Quintás-Cardama A, et al. Bone marrow stroma-secreted cytokines protect JAK2(V617F)-mutated cells from the effects of a JAK2 inhibitor. Cancer Res 2011;71:3831–40.

48. Agarwal A, Morrone K, Bartenstein M, Zhao ZJ, Verma A, Goel S. Bone marrow fibrosis in primary myelofibrosis: pathogenic mechanisms and the role of TGF-β. Stem Cell Investig 2016;3:5.

49. Zahr AA, Salama ME, Carreau N, et al. Bone marrow fibrosis in myelofibrosis: pathogenesis, prognosis and targeted strategies. Haematologica 2016;101:660–71.
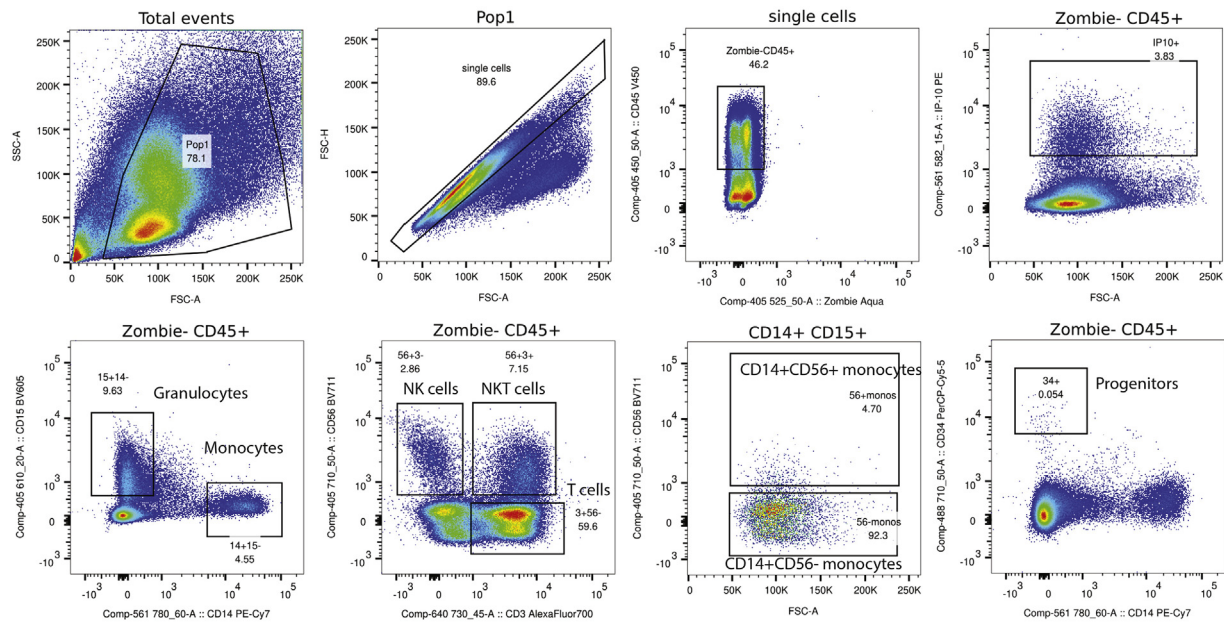
Supplementary Figure E1 Gate strategy used to identify IP-10-positive cells and leukocyte subsets granulocytes, CD14+CD56+ monocytes, CD14+CD56-monocytes, T-cells, NK-cells, NKT-cells, and progenitors [29].
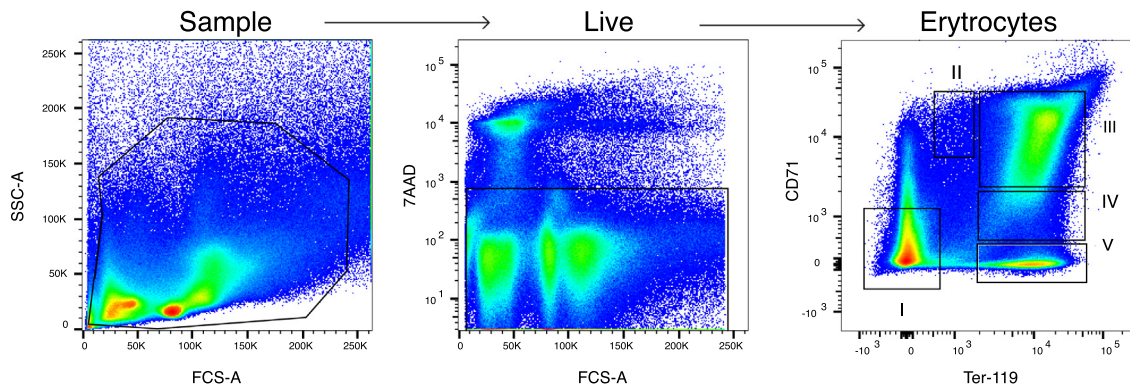

Supplementary Figure E2 Stages of erythroid differentiation (I through V) were defined based on CD71 and Ter-119 profiles. The precise borders between these regions were determined arbitrarily
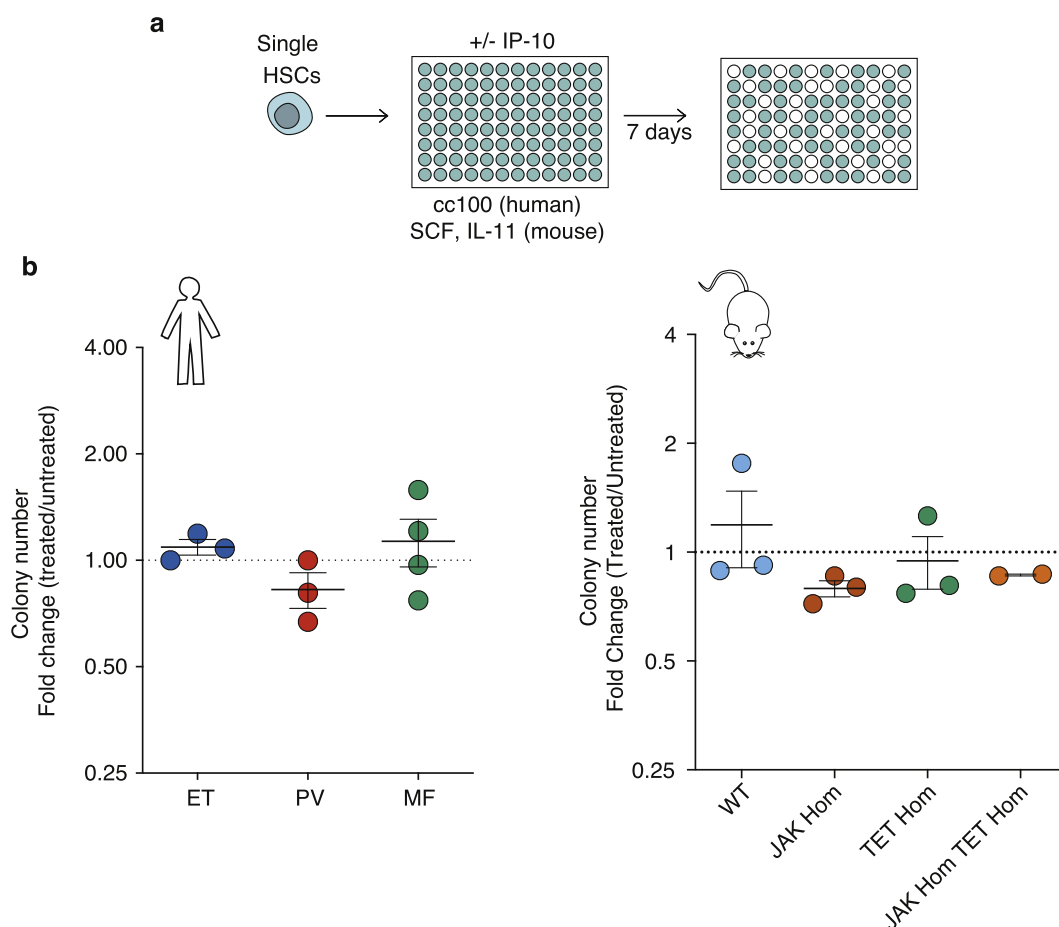
Supplementary Figure E3 a) Single HSCs were sorted from MPN patients (n = 3 ET, n = 3 PV, n = 4 MF) and from mouse models of MPNs (n = 3 WT, n = 3 JAK, n = 3 TET Hom, n = 2 JAK Hom TE2 Hom), cultured for 7 days with (Treated) or without (Untreated) IP-10 (50ng/mL and 100 ng/mL for human and mouse HSCs respectively) and assessed for cell survival. b) IP-10-treated HSCs did not show a significant difference in survival over the untreated counterparts. No differential effect of IP-10 was observed across the different MPN subtypes or MPN mouse models. Bars show mean with SEM.
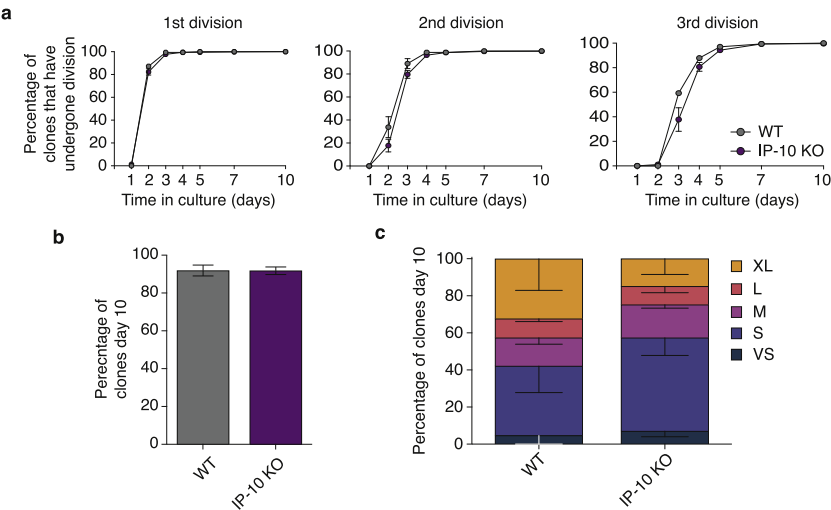
Supplementary Figure E4 a) Single CD45 + EPCR + CD48 - CD150 + Sca-1 high (ESLAM Sca-1high) LT-HSC from IP-10 KO (n = 3) and WT mice (n = 2) were sorted into individual wells of 96 well plates, cultured for 10 days in StemSpan with 10%FCS, 300ng/mL SCF, and 20ng/mL IL-11, and assessed for proliferation, cell cycle kinetics, and survival. IP-10 KO HSCs (purple line) do not have altered cell cycling compared to WT (grey line) HSCs. Two-way ANOVA (Sidak's multiple comparisons test). b) IP-10 KO (purple bar) and WT (grey bar) HSCs have comparable clone survival at day 1020post-isolation (Unpaired t-test, $p = 0.9801$). c) Colony size was measured on day 10 post- isolation and no differences in clone size distribution was observed between IP-10 KO and WT HSCs. Two-way ANOVA (Sidak's multiple comparisons test): VS = very small, $p = 0.9999$; S = small, $p = 0.7776$; M = medium, $p = 0.9998$; L = large, $p > 0.9999$; XL = very large, $p = 0.5105$. All bars show mean with SEM.
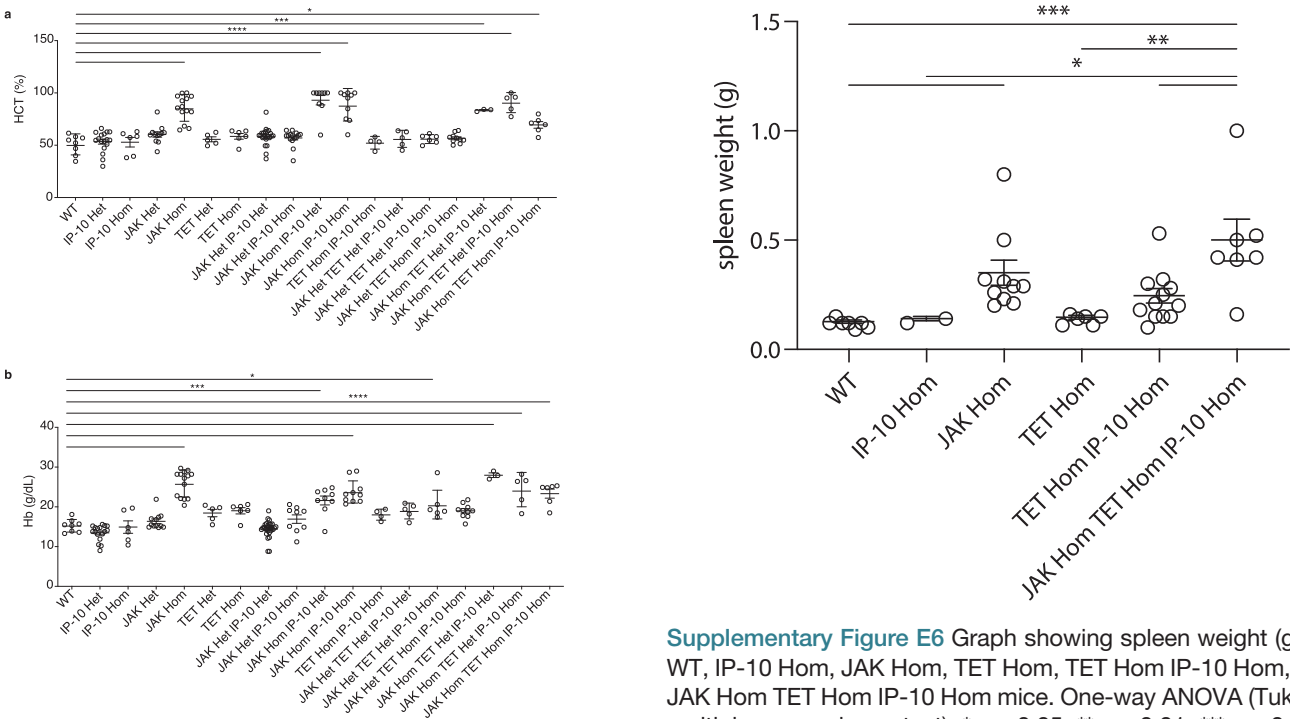
Supplementary Figure E5 Graphs showing a) HCT and b) Hb levels for WT, IP-10-mutated mice, JAK- IP-10-mutated mice, TET- IP-10-mutated mice and JAK- IP-10- TET-mutated mice. One-way ANOVA (Tukey's multiple comparisons test): *$p < 0.05$, **$p < 0.01$, ***$p < 0.001$, ****$p < 0.0001$. Comparisons shown for WT vs all other genotypes only. Bars show mean and SEM.

Supplementary Figure E6 Graph showing spleen weight (g) for WT, IP-10 Hom, JAK Hom, TET Hom, TET Hom IP-10 Hom, and JAK Hom TET Hom IP-10 Hom mice. One-way ANOVA (Tukey's multiple comparisons test): *$p < 0.05$, **$p < 0.01$, ***$p < 0.001$, ****$p < 0.0001$. Bars show mean and SEM.